The occurrence of through-bond orbital interactions in an α,ω donor–acceptor substituted bi(cyclohexylidene) and bi(cyclohexyl). X-Ray diffraction, UV–Vis absorption and photoelectron spectroscopy, *ab initio* SCF-MO and natural bond orbital analyses †

Wibren D. Oosterbaan,[a] Remco W. A. Havenith,[a,b] Cornelis A. van Walree,[a] Leonardus W. Jenneskens,*[a] Rolf Gleiter,[c] Huub Kooijman[d] and Anthony L. Spek[d]

[a] *Debye Institute, Department of Physical Organic Chemistry, Utrecht University, Padualaan 8, 3584 CH , Utrecht, The Netherlands. E-mail: jennesk@chem.uu.nl; Fax: +31-302534533; Tel: +31-302533128*

[b] *Debye Institute, Theoretical Chemistry Group, Utrecht University, Padualaan 8, 3584 CH, Utrecht, The Netherlands*

[c] *Institute of Organic Chemistry, University of Heidelberg, Im Neuenheimer Feld 270, 69120, Heidelberg, Germany*

[d] *Bijvoet Center for Biomolecular Research, Crystal and Structural Chemistry, Utrecht University, Padualaan 8, 3584 CH, Utrecht, The Netherlands*

Received (in Cambridge, UK) 14th March 2001, Accepted 15th May 2001
First published as an Advance Article on the web 11th June 2001

The ground state σ–π and π–π* interactions in 2-[4-(1-phenylpiperidin-4-ylidene)cyclohexylidene]malononitrile (**1**) and 2-[4-(1-phenylpiperidin-4-yl)cyclohexylidene]malononitrile (**2**) have been studied. Both the ionization potentials of **1** and **2**, and *ab initio* RHF/6-31G calculations in combination with a natural bond orbital analysis show that the ground state through-bond interaction (TBI) between the 1-phenylpiperidine electron donor and the dicyanoethylene electron acceptor in **1** and **2** is distinct but small. The olefinic bond in **1** enhances the interaction between the 1-phenylpiperidine electron donor and the dicyanoethylene electron acceptor as compared to **2**. The TBI between the *N*,*N*-dialkylanilino donor and the olefinic bond in **1** can be modulated by rotation of the phenyl group around the C–N bond. The solid state structures of **1** and **2** have been determined by single crystal X-ray diffraction. In the crystal intermolecular electron-donor–acceptor complexes are formed, which give rise to an intermolecular charge transfer absorption in the solid state.

Introduction

The process of (photoinduced) electron transfer forms the basis of an important and still expanding field of research. It is of fundamental interest in photosynthesis and molecular electronics.[1] Much insight has been gained by the experimental and theoretical study of (electron donor)–bridge–(electron acceptor) or D–B–A compounds[2] with saturated hydrocarbon bridges. An important role in the electron transfer process is reserved for the bridge. Hence, the development of bridges with optimized coupling between the functionalities is topical.[3]

One type of bridge that has been used[4] is based upon the oligo(cyclohexane-1,4-diylidene) skeleton, frequently dubbed oligo(cyclohexylidenes). Oligo(cyclohexane-1,4-diylidene)s are semi-rigid and possess an extended, rod-like geometry in which the cyclohexane-type rings adopt a chair-like geometry. Their length can be incremented in steps of about 4.1 Å. End-functionalized oligo(cyclohexane-1,4-diylidene)s[5] have been shown to be suitable as molecular building blocks for use in supramolecular assemblies like Langmuir–Blodgett mono- and multilayers transferred to silicon (100) surfaces[6] and non-covalent polymers.[7] Self-assembled monolayers of sulfide end-functionalized oligo(cyclohexane-1,4-diylidene) derivatives have recently been used as rigid spacers in a study of photo-induced electron transfer between CdSe quantum dots and a gold surface.[8]

An interesting property of oligo(cyclohexane-1,4-diylidene)s is their alternating σ–π topology. It has been shown by photo-electron spectroscopy (PES) in combination with *ab initio* calculations that significant ground state through-bond electronic interactions occur between *a* and *ω* substituents of appropriately *a*,*ω*-substituted oligo(cyclohexane-1,4-diylidene)s (Chart 1)[9] while in the corresponding *a*,*ω*-substituted bi(cyclohexyl)s

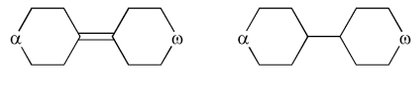

(*a*) (*b*)

Chart 1 *a*,*ω*-Substituted bi(cyclohexylidene)s (*a*) and bi(cyclohexyl)s (*b*).

they are very small.[10] Thus, it is expected that the presence of an olefinic bond in the saturated hydrocarbon bridge enlarges the ground state interaction between D and A which in turn promotes the coupling between the D–B–A and $D^{\bullet+}$–B–$A^{\bullet-}$ states, thus affecting the rate constants of (photoinduced) charge separation and recombination processes. Therefore, it is

† Electronic supplementary information (ESI) available: photoelectron spectra of **8** and **5** (Fig. 1S and 2S) and NBO interaction diagrams for **5** (C_1) (Fig. 3S), **1** (C_S) (Fig. 4S), **1** ⊥ (C_S) (Fig. 5S), **1** ax (C_S) (Fig. 6S), **2** eq (Fig. 7S) and **2** ⊥ (C_S) (Fig. 8S). See http://www.rsc.org/suppdata/p2/b1/b102410h/

 DOI: 10.1039/b102410h

Table 1 Crystallographic data for **1** and **2**

Compound	**1**	**2**
Formula	$C_{20}H_{21}N_3$	$C_{20}H_{23}N_3$
M_r	303.40	305.41
Crystal system	Monoclinic	Monoclinic
Space group	$P2_1/m$ (No. 11)	$P2_1/m$ (No. 11)
Z	2	2
a/Å	7.0681(12)	7.0137(10)
b/Å	11.9013(12)	11.941(2)
c/Å	9.3556(12)	9.6449(17)
β/°	90.931(7)	92.286(11)
V/Å^3	786.89(19)	807.1(2)
T/K	125	150
$D_{calc.}$/g cm^{-3}	1.281	1.257
$\mu_{calc.}$/mm^{-1} (Mo-Kα)	0.08	0.08
Measured refl.	4846	4551
Independent refl., R_{int}	1871, 0.0384	1724, 0.0446
R^a	0.0396 [1492 $I > 2\sigma(I)$]	0.0545 [1346 $I > 2\sigma(I)$]
$wR2^b$	0.1112	0.1277
GoF	1.047	0.954

[a] $R = \Sigma||F_o| - |F_c||/\Sigma|F_o|$. [b] $wR2 = [\Sigma[w(F_o^2 - F_c^2)^2]/\Sigma[w(F_o^2)^2]]^{1/2}$.

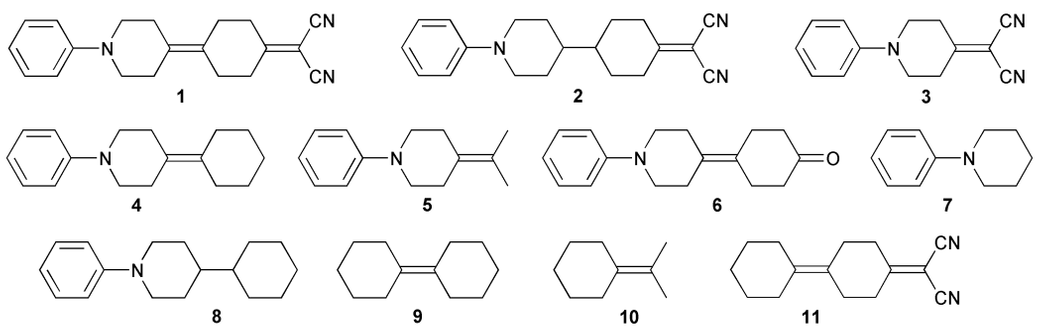

Chart 2 Compounds under investigation.

of interest to study the possible occurrence of ground state interactions in the corresponding donor–acceptor molecules **1** and **2** (Chart 2). In these molecules the anilino moiety acts as an electron donor and the dicyanoethylene moiety as an electron acceptor. Upon excitation the formation of a charge separated state was detected for both molecules.[4a] Interestingly, it was found that the rate of charge recombination in **1** was about a factor of 20 higher than in **2** which was thought to be the result of a significantly enlarged electronic coupling between D–B–A and $D^{\bullet+}$–B–$A^{\bullet-}$ in **1**.

Although in the excited state the effect of the presence of a double bond is thus manifest, the role of the double bond in the ground state is not clear. In this study the occurrence of ground state electronic interaction between the chromophores in **1** and **2** is evaluated experimentally in the solid state and in the gas phase using single crystal X-ray diffraction, electronic absorption spectroscopy and photoelectron spectroscopy in combination with natural bond orbital (NBO) analyses, respectively.

Results and discussion

Single crystal X-ray structures of 1 and 2

The molecular structures of **1** and **2** were determined by single crystal X-ray diffraction. Both crystallize in the $P2_1/m$ space group and their crystal data are given in Table 1. ORTEP representations of **1** and **2** are shown in Fig. 1 and salient structural data (bond lengths, valence angles) are presented in Tables 2 and 3. In addition the structures of **1** and **2** were optimized at the RHF/6–31G level of theory (see below and also Tables 2 and 3). A satisfactory agreement was obtained between the X-ray and calculated data.

In both **1** and **2** the cyclohexane-type rings adopt a chair-type

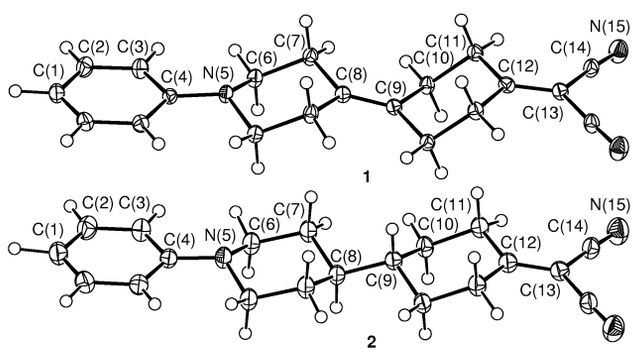

Fig. 1 ORTEP drawings of the X-ray structures of **1** and **2** made with PLATON.[18] Displacement ellipsoids at the 50% probability level are shown.

conformation ‡[11] as was earlier found for 4-(1-phenylpiperidin-4-ylidene)cyclohexanone (**6**),[12] an analogue of **1**, which contains a carbonyl moiety instead of the dicyanoethylene acceptor. Although the phenyl group in **1** and **2** (as well as in **6**) adopts an equatorial orientation, it should be noted, that for the related compound **3** the phenyl group has been found to occupy an axial orientation.[13] Initially this was thought to be the consequence of a stabilization in the solid state of this conformer due to optimal TBI between donor and acceptor.[13] Ogawa *et al.*,[14] however, concluded that the preferred geometry around the N atom in *N*-arylpiperidines in the solid state is primarily determined by intermolecular interactions.

‡ Cremer and Pople[11] parameters θ found for **1** are: 5.1(1)° [N(5)–C(6)] and 7.2(1)° [C(9)–C(12)]. For **2** these are 3.3(2)° [N(5)–C(8)] and 16.3° [C(9)–C(12)]. A perfect chair conformation has $\theta = 0°$.

Table 2 Selected bond lengths (Å) in **1** and **2** in the crystal structures and their C_s symmetry optimized RHF/6-31G geometries. Values corresponding to comparable bond lengths in the two structures of **6** (both C_1 symmetry) are also given

	1		**2**		**6** A	**6** B
Bond	Crystal	Calc.	Crystal	Calc.	Crystal	Crystal
C(1)–C(2)	1.3832(13)	1.3847	1.388(2)	1.3846	1.373(4); 1.381(4)	1.375(4); 1.373(4)
C(2)–C(3)	1.3909(15)	1.3853	1.389(2)	1.3853	1.374(4); 1.375(4)	1.383(3); 1.381(4)
C(3)–C(4)	1.4072(13)	1.4033	1.408(2)	1.4035	1.398(3); 1.403(4)	1.398(3); 1.403(3)
C(4)–N(5)	1.4072(18)	1.4095	1.410(3)	1.4088	1.413(3)	1.413(3)
N(5)–C(6)	1.4659(12)	1.4609	1.466(2)	1.4602	1.465(3); 1.460(3)	1.462(3); 1.459(3)
C(6)–C(7)	1.5319(15)	1.5344	1.529(2)	1.5287	1.513(3); 1.512(3)	1.517(3); 1.521(3)
C(7)–C(8)	1.5100(13)	1.5108	1.528(2)	1.5350	1.513(3); 1.504(3)	1.509(3); 1.507(4)
C(8)–C(9)	1.3450(19)	1.3351	1.541(3)	1.5501	1.327(3)	1.335(3)
C(9)–C(10)	1.5103(13)	1.5169	1.525(2)	1.5414	1.506(3); 1.517(4)	1.506(4); 1.514(3)
C(10)–C(11)	1.5523(15)	1.5475	1.540(2)	1.5419	1.529(4); 1.519(4)	1.527(4); 1.529(4)
C(11)–C(12)	1.4958(13)	1.5048	1.496(2)	1.5033	1.503(4); 1.488(4)	1.504(4); 1.492(4)
C(12)–C(13)	1.358(2)	1.3456	1.355(3)	1.3452		
C(13)–C(14)	1.4414(13)	1.4339	1.437(2)	1.4338		
C(14)–N(15)	1.1476(14)	1.1474	1.150(2)	1.1474		

Table 3 Selected bond angles (°) in the crystal structures of **1** and **2** and in their C_s symmetry optimized RHF/6-31G geometries. Values corresponding to comparable angles in the two structures of **6** are also given

	1		**2**		**6** A	**6** B
Bond angle	Crystal	Calc.	Crystal	Calc.	Crystal	Crystal
C(1)–C(2)–C(3)	121.17(10)	121.27	121.02(19)	121.28	120.9(2); 120.6(2)	121.4(2); 121.0(2)
C(2)–C(1)–C(2)A	118.53(12)	118.05	118.5(2)	118.03	119.0(2)	118.5(2)
C(2)–C(3)–C(4)	121.09(10)	121.37	121.35(17)	121.40	121.2(2); 121.1(2)	120.9(2); 121.2(2)
C(3)–C(4)–C(3)A	116.93(11)	116.66	116.79(17)	116.61	117.0(2)	116.8(2)
C(3)–C(4)–N(5)	121.47(6)	121.67	121.55(10)	121.69	120.2(2); 122.7(2)	120.8(2); 122.3(2)
C(4)–N(5)–C(6)	118.93(6)	119.59	117.15(11)	119.82	116.06(18); 118.05(19)	117.62(18); 117.95(19)
C(6)–N(5)–C(6)A	111.96(9)	112.44	113.15(16)	113.78	110.99(17)	111.29(17)
C(6)–C(7)–C(8)	113.15(9)	111.74	113.14(15)	112.90	112.1(2); 114.0(2)	113.7(2); 112.9(2)
C(7)–C(8)–C(7)A	111.00(10)	108.56	107.17(15)	106.92	110.68(19)	110.9(2)
C(7)–C(8)–C(9)	124.47(6)	125.72	112.02(11)	112.65	123.8(2); 125.5(2)	124.4(2); 124.6(2)
C(8)–C(9)–C(10)	124.49(6)	124.68	112.85(11)	111.97	125.4(2); 123.8(2)	124.6(2); 124.4(2)
C(9)–C(10)–C(11)	110.58(9)	111.60	111.55(14)	112.93	111.1(2); 112.3(2)	110.7(2); 111.5(2)
C(10)–C(9)–C(10)A	110.95(10)	110.64	108.09(15)	109.15	110.8(2)	111.0(2)
C(10)–C(11)–C(12)	110.62(9)	110.89	113.08(15)	111.00	111.9(2); 111.7(2)	111.8(2); 111.3(2)
C(11)–C(12)–C(11)A	116.11(11)	114.17	116.87(16)	113.61	114.7(2)	114.5(2)
C(11)–C(12)–C(13)	121.93(6)	122.91	121.49(9)	123.19		
C(12)–C(13)–C(14)	123.23(6)	122.23	122.89(9)	122.19		
C(13)–C(14)–N(15)	175.89(11)	179.55	176.57(17)	179.52		
C(14)–C(13)–C(14)A	113.52(11)	115.54	114.22(16)	115.61		
$\Sigma\theta_i$/°	349.82(12)	353.80	347.4(2)	353.42	345.1(3)	346.9(3)
τ/°	30.16(13)	23.89	34.1(2)	24.45	36.6(2)	34.3(2)

In order to compare the configuration of the piperidino nitrogen atom for **1** and **2** two parameters are introduced which describe the degree of pyramidalization;[14] (1) the sum of the bond angles around the N atom, $\Sigma\theta_i$, which should be ~328.4° for a purely tetragonal sp^3 geometry and 360° for a purely trigonal sp^2 geometry, and (2) the angle τ, which is defined as the angle between the plane through C(6), N(5) and C(6A) and the N(5)–C(4) bond (Fig. 2). The angle τ is 0° for an sp^2 nitrogen atom and ~60° for an sp^3 nitrogen atom. From the values of $\Sigma\theta_i$ and τ it can be deduced that the degree of pyramidalization in the crystal structures of **1**, **2** and the two molecules found in the structure of **6** is similar (Table 3).

A remarkable point in the crystal structures of **1** and **2** is their molecular C_s symmetry, *i.e.* the phenyl group in these molecules is *not* rotated around the C–N bond. Generally, the phenyl group in *N*-phenylpiperidines is rotated around the C–N bond by a twist angle θ (Fig. 2). For instance, using PES for 1-phenylpiperidine (**7**) in the gas phase a preferred twist angle θ of 48° was inferred.[15] The twist angles for the two crystallographically independent molecules found in the unit cell of **6** are 17.4 and 26.5°, respectively.[12] For comparison, the structures of **1** and **2** were optimized at the *ab initio* RHF/6-31G level of theory with and without a C_s constraint. At this level of theory the preferred twist angle θ is ~42° (Table 4), which is in accordance with the value found for **7** in the gas phase. Under the constraint of C_s symmetry, the calculated structures for **1** (C_s) and **2** (C_s) are positioned only 2.4 and 2.5 kcal mol^{-1} higher in energy, respectively. These geometries were characterized as transition states for rotation around the phenyl C–N bond [−67.4 cm^{-1} for **1** (C_s) and −78.7 cm^{-1} for **2** (C_s)]. The bond lengths and valence angles of the C_s symmetric structures are in satisfactory agreement with those found in the solid state (Tables 2 and 3). An explanation for the presence of the 'gas phase' transition state geometry in the solid state is provided by the fact that the *N*,*N*-dialkylanilino moieties of **1** and **2** form charge transfer (CT) complexes with the dicyanoethylene groups of neighbouring molecules (see below).

The molecules in the crystal structures of **1** and **2** are arranged in a head-to-tail fashion. In both cases the π system of the dicyanoethylene moiety of one molecule and the dialkylanilino unit of another molecule are positioned in a *co*-facial arrangement (Fig. 3). Interestingly, these intermolecular CT complexes are not present in the crystal structure of **6**, where all carbonyl moieties are stacked above each other and are accompanied by hydrogen bonds with axial hydrogen atoms.[12] The stabilizing interaction[16] due to the formation of the complexes probably accounts for the difference in packing from that observed for **6**. The packing of **1** and **2** (both containing one

Table 4 Values for $\Sigma\theta_i$, θ, relative total energies E_{rel} (kcal mol^{-1}) and orbital energies $-\varepsilon_j$ of the RHF/6-31G optimized geometries of (conformers of) **1**, **2**, **4**, **5**, **7**, **8**, **9**, **10** and **11**. The energy of the lowest energy conformer was set to zero

					$-\varepsilon_j$/eV					
Compound	Symmetry	$\Sigma\theta_i$/°	θ/°	E_{rel}	Lp–π_{ar}	π_c	π_{ar}	π_{ar}–Lp	π_{acc}	σ
1	C_1	351.22	42.33	0	8.14	9.40	9.26	10.78	10.40	12.07
1	C_s	353.80	0	2.4	7.77	9.46	9.22	11.25	10.45	12.08
1 ⊥	C_s	347.16	90	0.9	9.14 (π_{ar})	9.23	9.30	9.78 (Lp)	10.40	12.01
1 ax	C_s	356.46	0	3.0	7.60	9.49	9.25	11.33	10.43	12.09
2	C_1	350.85	41.74	0	8.08		9.23	10.60	10.28	11.95
2	C_s	353.42	0	2.5	7.71		9.18	11.08	10.31	11.95
2 ⊥	C_s	346.03	90	0.8	9.09 (π_{ar})		9.26	9.56 (Lp)	10.26	11.89
2 ax	C_s	356.16	0	2.8	7.57		9.20	11.00	10.30	11.98
4	C_1	351.36	41.73	0	7.79	8.66	9.02	10.42		11.14
5	C_1	351.50	40.90	0	7.79	8.73	9.02	10.45		11.68
5	C_s	353.65	0	2.2	7.46	8.81	8.97	10.90		11.70
7	C_1	351.36	41.98	0	7.81		9.01	10.31		12.09
8	C_1	350.70	40.69	0	7.79		9.01	10.30		11.04
9[21b]	C_{2h}					8.48				10.89
10	C_1					8.45				11.25
11	C_s					9.26			10.36	11.71

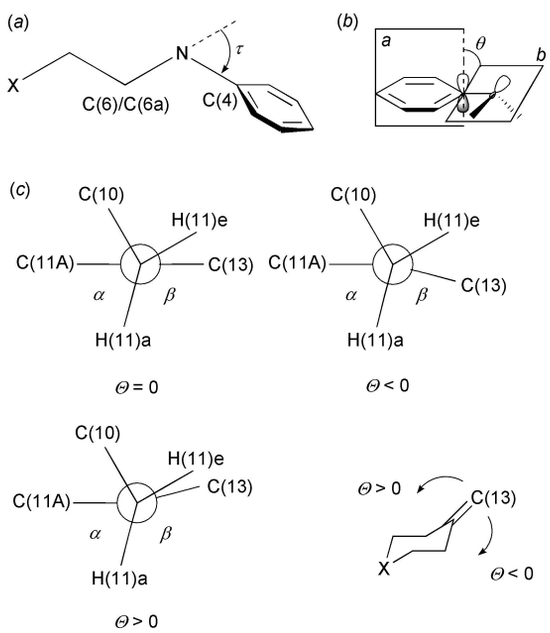

Fig. 2 (*a*) Definition of the angle τ. (*b*) Graphical representation of the twist angle θ as the angle between planes *a* and *b* in an *N*,*N*-dialkylaniline. Plane *a* is the plane perpendicular to the benzene ring and through the C(4)–N(5) bond. Plane *b* is the plane through the same C–N bond and through the axis of the lone pair on nitrogen. (*c*) Newman projections along the C(11)–C(12) bond for different signs of the value of Θ, which is defined[13] as $\Theta = (\alpha + \beta) - 180$.

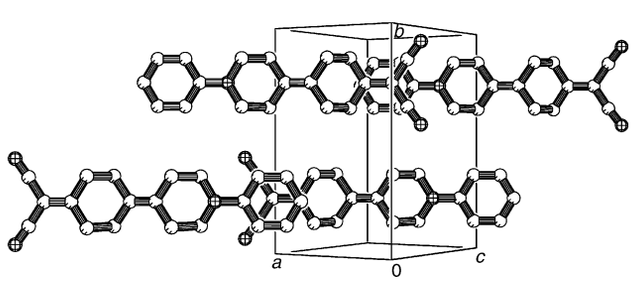

Fig. 3 Stacking of four molecules of **1** in the unit cell. The view is perpendicular to a plane through C(1), C(3) and C(3A). Hydrogen atoms are omitted for clarity.

crystallographic independent molecule) is more efficient than in that of **6** (containing two independent molecules) as indicated by the packing coefficient *k* (calculated according to Kitaigorodskii[17] using the VOID option of PLATON[18]) which amounts

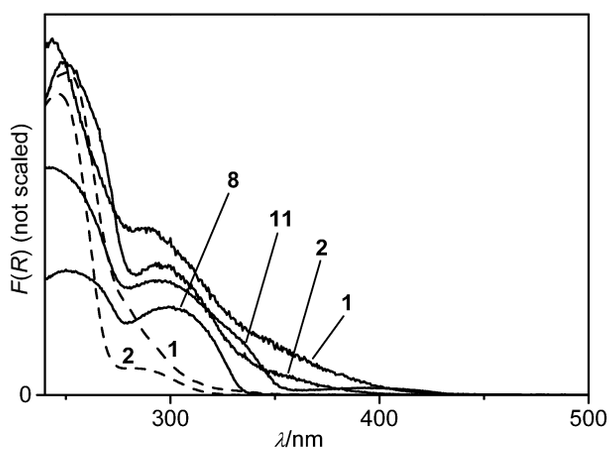

Fig. 4 Solid state UV–Vis absorption spectra (solid lines) of dispersions of **1**, **2**, **8** and **11** in KBr (ordinate in Kubelka Munk units) together with solution spectra[4a] (dotted lines) of **1** and **2** in cyclohexane.

to 0.729 and 0.723 for **1** and **2** respectively, while for **6** a lower value of 0.686 is found. The closest distance between the two co-facial π systems in the structures of **1** and **2**, taken as the distance between the atoms C(1) and C(12), is 3.455(2) Å for **1** and 3.560(4) Å for **2**. The distances between atoms C(3) and C(14) amount to 3.6983(16) Å and 3.841(2) Å for **1** and **2**, respectively. As indicated by these distances, the π complex of **1** is stronger than that of **2**.

Solid state UV–Vis absorption spectroscopy

Solid-state UV–Vis diffuse reflectance spectra were recorded of **1**, **2**, 1-phenyl-4-cyclohexylpiperidine (**8**) and 2-[1,1′-bi(cyclohexyliden)-4-ylidene]malononitrile (**11**) dispersed in solid KBr. The spectra are presented in Fig. 4 along with solution spectra of **1** and **2** in cyclohexane. In addition to all absorption bands found in the solution spectra, in the solid state **1** and **2** exhibit an additional absorption tail above 350 nm, which is present neither for **8** and **11** in the solid state nor for **2** in solution. These tails visible in the case of **1** and **2** in the solid state are likely to stem from an intermolecular CT absorption and demonstrate the occurrence of intermolecular CT interactions in the solid state (Fig. 3).

A close inspection of the spectra in Fig. 4 reveals that the CT absorption in **1** is more intense and slightly red-shifted as compared to that found for **2**. This is expected on account of the closer (intermolecular) proximity of the donor and acceptor in **1** in comparison to **2** in the solid state (see above). A

Table 5 Vertical ionization energies $I_{v,j}$ from PES, RHF/6-31G orbital energies $-\varepsilon_j$ and assignments for **1**, **4**, **5** and **8**

Compound	Band (j)	$I_{v,j}$/eV	$-\varepsilon_j$/eV	Assignment
1 (C_1)	1	7.6	8.14	81a π_{ar}–Lp
	2	8.9[a]	9.26	80a π_{ar}–π_c
	3		9.40	79a π_c–π_{ar}–π_{acc}
	4	9.8[a]	10.40	78a π_{acc}–π_c–Lp
	5		10.78	77a π_{ar}–Lp
	6	10.4	12.07	76a σ
	7	—	13.03	75a σ
4 (C_1)	1	7.4	7.79	66a π_{ar}–Lp
	2	8.3	8.66	65a π_c
	3	8.9	9.02	64a π_{ar}
	4	9.8[a]	10.42	63a Lp–π_{ar}
	5		11.14	62a σ
5(C_1)	1	7.5	7.79	55a π_{ar}–Lp
	2	8.3	8.73	54a π_c
	3	8.9	9.02	53a π_{ar}
	4	9.6	10.45	52a Lp–π_{ar}
	5	10.4	11.68	51a σ
8 (C_1)	1	7.36	7.79	67a π_{ar}–Lp
	2	8.97	9.01	66a π_{ar}
	3	—	10.30	65a Lp–π_{ar}
	4	—	11.04	64a σ

[a] Overlap of bands.

contribution of an intramolecular absorption to the spectrum of **1** can however not be excluded. Interestingly, **1** exhibits a (very) weak absorption band in cyclohexane solution (estimated maximum at *ca.* 300 nm) extending to 350 nm. This absorption is neither present in the spectrum of **11** nor in that of **4** and is attributed to an intramolecular transition involving charge transfer from the dialkylanilino donor to the dicyanoethylene acceptor.[19] For **2** such an intramolecular CT absorption is absent.

The fact that in the solid state a CT absorption is found for **2** which is absent in solution, suggests that intermolecular through-space (TS) orbital interactions between the donor and acceptor moieties in the crystals of **1** and **2** are much larger than the intramolecular interaction between donor and acceptor. Hence in the solid state the orbital interactions in the case of **1** and **2** are primarily of an intermolecular nature and hamper the detection of possible weak intramolecular interactions mediated by the hydrocarbon bridge.

Photoelectron spectroscopy of 1 and 2

To gain insight into the occurrence of possible weak interactions we focussed our attention on PES and *ab initio* quantum chemical calculations. By a combination of these methods it has been shown that in α,ω-bifunctionalized oligo(cyclohexane-1,4-diylidene)s sizable electronic interactions between the α and ω substituents and part of the cyclohexane based orbitals mediated by the central olefinic bond can be present.[9a,10] This occurs in particular when the interacting orbitals of the functionalities and the central olefinic bond of the bridge possess similar self-energies and then only when they belong to the same irreducible representation. To probe the occurrence of ground state TB or TS orbital interactions between the chromophores in **1** and **2** in the gas phase, a He (I) PES study was performed.

The He (I) photoelectron (PE) spectra are analysed using the following procedure. Firstly, the observed PE bands of **1**, **4**, **5**, and **8** are correlated with those of model compounds. Secondly, the experimental vertical ionization potentials $I_{v,j}$ are correlated with *ab initio* molecular orbital energies using Koopmans' theorem ($I_{v,j} = -\varepsilon_j$).[20] The TB and TS orbital interactions between the chromophores are subsequently assessed by means of natural bond orbital (NBO) analyses.

Selected geometrical data on the optimized geometries of **1**, **4**, **5**, **8** and some model compounds are given in Table 4. The $I_{v,j}$ values for **1**, **4**, **5** and **8** are given in Table 5 together with RHF/6-31G orbital energies $-\varepsilon_j$ and their assignments.§[21] Unfortunately, due to its low vapour pressure the PE spectrum of **2** could not be recorded. In the PE spectrum of **8** (Supplementary Data, Fig. 1S) the two bands with lowest energy can be associated with the first two bands found in the PE spectrum of 1-phenylpiperidine (**7**), for which three bands positioned at 7.72, 9.09 and 9.72 eV were found.[15] The first and third bands of **7** were assigned to the two linear combinations of one of the two degenerate $\pi(e_{1g})$ HOMO's of benzene with the nitrogen lone pair Lp (Lp–π_{ar} and π_{ar}–Lp).¶[22] The second band was assigned to the benzene $\pi(e_{1g})$ MO with a nodal plane running through nitrogen. The third band of **8**, associated with the π_{ar}–Lp MO, overlaps with one or more bands associated with 'ribbon-type'[23] σ MO's of the saturated hydrocarbon skeleton. These MO's are positioned at higher energy than those of **7** due to the larger extension of the saturated hydrocarbon skeleton.[23b]

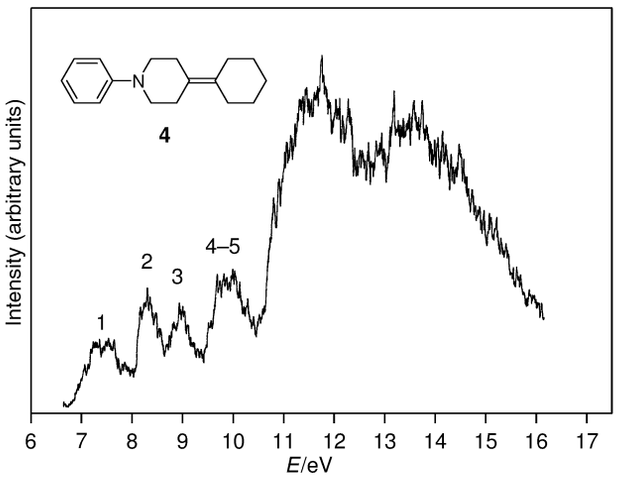

Fig. 5 Photoelectron spectrum of **4**.

The PE spectrum of **4** is depicted in Fig. 5. The double bond π_c in **4** does not significantly influence the position of the two lowest energy bands of the *N*,*N*-dialkylaniline chromophore. Its $I_{v,j}$ value (8.3 eV) is shifted to higher energy by 0.1(4) eV (calculated shift: 0.18 eV, Table 4) as compared to its position[9a] in bi(cyclohexylidene) (**9**, 8.16 eV). As shown below, the NBO analysis of **4** shows that this can be attributed to an inductive shift.‖ The broad band at 9.8 eV is associated with the overlapping bands belonging to ribbon σ MO's and the π_{ar}–Lp MO. For **9** the highest energy ribbon MO-type band is positioned at 9.80 eV,[9a] also well separated from the σ manifold. The PE spectrum of **5** (Supplementary Data, Fig. 2S), which has a smaller hydrocarbon skeleton so that the σ ribbon MO is located at lower energy ($I_{v,j}$ = 10.4 eV) and does not overlap anymore with the Lp–π_{ar} band ($I_{v,j}$ = 9.6 eV), supports this assignment. A comparison with the $I_{v,j}$ values of **7** (see above) and isopropylidenecyclohexane (**10**), for which a value of 8.34 eV for the $I_{v,j}$ of the double bond has been reported,[24] suggests that for **5**, as for **4**, interactions between the *N*,*N*-dialkylanilino chromophore and the double bond are small.

The PE spectrum of **1** is shown in Fig. 6. The very broad band at 7.6 eV (π_{ar}–Lp MO) is shifted to higher energy in comparison with the same band in **4** and **5** by 0.2 eV due to an inductive

§ In previous papers we have shown that RHF/6-31G[21a] calculations give a good description of the energies and order of valence occupied molecular orbitals of bi(cyclohexylidene)[21b,c] and various end-functionalized derivatives.[9a,10] Re-optimization at the RHF/6-31G* or RHF/6-311G** levels of theory gave nearly identical results for the energies and order of the occupied valence molecular orbitals.

¶ The splitting between these two bands has been used to assess the resonance interaction between the lone pair on nitrogen and the π-electrons on the phenyl ring.[15,22]

‖ The ionization energy of the σ skeleton will shift by −0.1(4) eV, which is difficult to observe because of band overlap.

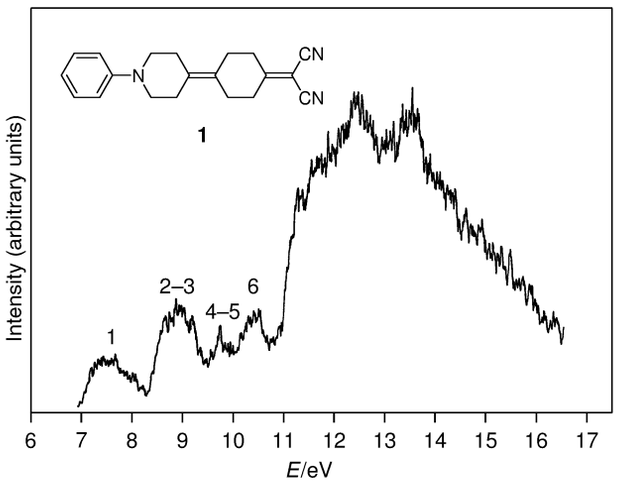

Fig. 6 Photoelectron spectrum of **1**.

shift (calculated shift: 0.35 eV).** The broad band at 8.9 eV is composed of two peaks, one presumably of the double bond and one of the π_{ar} MO of the *N*,*N*-dialkylanilino moiety. Between 9.5 and 10.8 eV three bands are expected on the basis of the calculations and correlation with related compounds (**4**, **5**, **11**). The band (6) at 10.4 eV is associated with ribbon type σ MO's by correlation with corresponding bands in **5** (10.4 eV) and **11**[10] (10.3 eV). The bands expected for the π_{ar}–Lp MO and the $\pi(C{=}C(CN)_2)$ MO overlap considerably around 10 eV. Nevertheless, on the basis of the 7.6 eV and broad 8.9 eV bands (the latter consisting of two superimposed bands), it can be concluded that the PE spectrum of **1** is virtually a superposition of those of **7** and **11**. Hence, supported by the PE measurements and calculations it is concluded that TBI between these two parts of the molecule is very small.

NBO analyses

The occurrence of TB and TS interactions in **1**, **2** and **4** was probed by means of NBO analyses using the definition of TBI given by Hoffmann.[25] To determine the interaction between (localized) chromophores, the RHF/6-31G wavefunctions were subjected to a Weinhold natural bond orbital (NBO) localization procedure.[26] The canonical molecular orbitals (CMO's) were transformed into an orthonormal set of localized NBO's, which represent formal core s orbitals, σ, σ*, π and π* orbitals, lone pairs and Rydberg orbitals. The contribution of an NBO or a set of NBO's forming a precanonical MO (PCMO) to the energy of the CMO's can then be evaluated.

It has been found previously[9a,10] that in *α*,*ω*-end-functionalized oligo(cyclohexane-1,4-diylidene)s with π type functionalities, the main contribution of TB interaction is mediated by the H_{ax}–C–C–H_{ax} PCMO's in between the two π systems. The compounds on which this conclusion was based were more symmetrical (C_{2h}) than the compounds under study here. Due to this lack of symmetry the contribution to TBI of NBO's other than those present in the H_{ax}–C–C–H_{ax} PCMO's is enlarged. Therefore it is not straightforward anymore to select a subset of NBO's responsible for TBI and we choose to use all NBO's in order to be able to compare the affects of TBI independently of the chosen set.

NBO analysis of 4. In Fig. 7 the NBO interaction diagram of **4** is shown. In step 1 the highest energy levels of the phenyl π system PCMO's (π_{ar}: −8.90 and −9.01 eV), the self-energy of the olefinic π NBO (π_c: −9.44 eV) and the self-energy of the nitrogen lone pair NBO (Lp: −10.25 eV) are shown. In step 2 interactions between the nitrogen lone pair and the phenyl π system are allowed, giving the two linear combinations π_{ar}–Lp and Lp–π_{ar}. When the π_c NBO and the *N*-phenyl π system are allowed to interact mutually, the energy levels do not change, leading to the conclusion that TS interaction is negligible.[27]

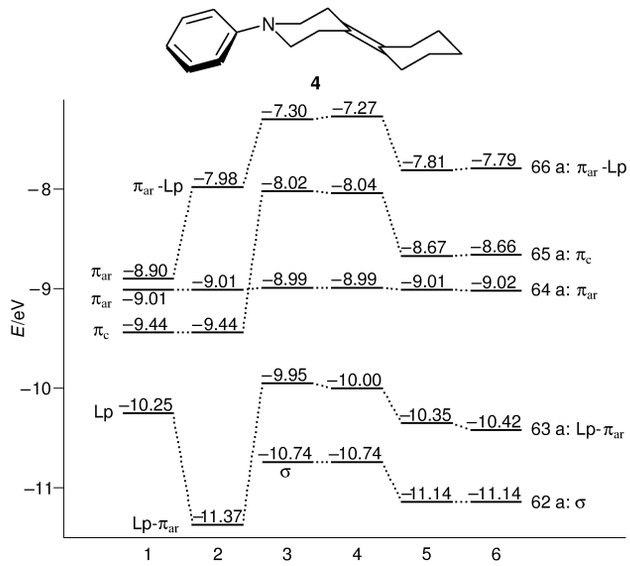

Fig. 7 TS–TB interaction diagram (RHF/6-31G NBO analysis) of **4**. For a description of the steps: see text.

In step 3, the π_c NBO and the *N*-phenyl π system are both allowed, albeit independently, to interact with *all* bonding C–C, C–N and C–H σ NBO's. This strongly destabilizes all PCMO's, with the exception of the π_{ar} PCMO due to its nodal character.

In step 4 a simultaneous interaction between the π_c NBO, the *N*-phenyl π system PCMO's and the aforementioned σ orbitals is allowed. A small TB interaction between the chromophores is present, destabilizing the π_{ar}–Lp PCMO by 0.03 eV, while stabilizing the levels of the π_c NBO and the Lp–π_{ar} PCMO by 0.02 and 0.05 eV, respectively. This minute TB interaction is mainly relayed by the H_{ax}–C–C–H_{ax} PCMO's in between the two π systems.

In order to test whether the TB interactions found in going from step 3 to step 4 are affected by addition of antibonding and Rydberg NBO's steps 3 and 4 were repeated in steps 5 and 6 with an enlarged set of NBO's comprising also the mentioned antibonding and Rydberg NBO's. The results show that the influence of the antibonding and Rydberg NBO's in mediating TBI is negligible since the changes in the energy levels remain the same.

One should realize that the energy of the π_c level in **4** is not indicative of the occurrence of TBI. Whereas the π_c level is lowered in energy by TBI with the π_{ar}–Lp level, it can be raised by TBI with the Lp–π_{ar} level. Hence, to probe possible TB interactions involving π_c the change in energy of the π_{ar}–Lp and Lp–π_{ar} levels should be monitored. Indeed a weak TBI between the *N*-phenyl π system and π_c is present [$\Delta E(\pi_{ar}\text{–Lp}) = 0.03$eV; $\Delta E(\text{Lp–}\pi_{ar}) = -0.05$ eV]. However, the overall effect on the π_c CMO energy [$\Delta E(\pi_c) = -0.02$ eV] is insignificant with respect to the difference of 0.18 eV between the CMO energy of π_c in **9** and **4**, which thus predominantly arises from an inductive shift (Tables 4 and 5). A similar MO interaction diagram was obtained for 1-phenyl-4-(isopropylidene)piperidine (**5**) (Supplementary Data, Fig. 3S).

NBO analysis of 1. The NBO interaction scheme for **1** (C_1 symmetry) is depicted in Fig. 8. In addition to the levels already present in **4**, the π_{acc} level due to the π system of the dicyanoethylene acceptor is present. Step 2 allows the interaction

** It is known that as a consequence of the introduction of a dicyanoethylene moiety the ionization potential of the olefinic bond in **11** is inductively raised by *ca.* 0.6 eV compared to **9**.[10] Calculations presented in ref. 10 indicate, however, that a substantial amount of TBI is present in **11**, probably contributing to the 0.6 eV shift.

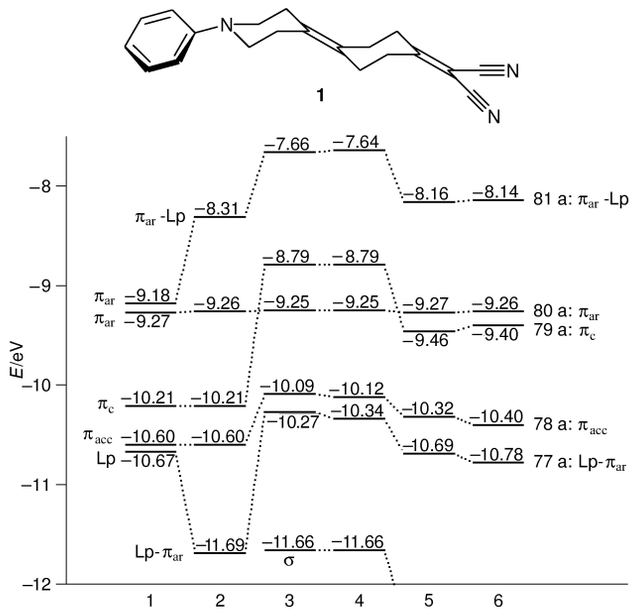

Fig. 8 TS–TB interaction diagram (RHF/6-31G NBO analysis) of **1**. For a description of the steps: see text.

between the phenyl π system and the lone pair on nitrogen (Lp). As expected TS interaction between the anilino group, π_c and π_{acc} was found to be negligible. Step 3 shows to what extent the π systems interact with the σ NBO's of the hydrocarbon skeleton. In step 4 TB interaction between all π systems is allowed. The Lp–π_{ar} PCMO and the π_{acc} PCMO are slightly stabilized [ΔE(Lp–π_{ar}) = −0.07 eV; $\Delta E(\pi_{acc})$ = −0.03 eV], indicating that some interaction between the π_c level, of which the energy again does not change, and the chromophores at the termini of the molecule is present. The effect becomes more pronounced when going from step 5 to 6, when antibonding and Rydberg NBO's are allowed to participate in TBI {step 3 to 4 [5 to 6]: ΔE(Lp–π_{ar}) = −0.07 [−0.09] eV and $\Delta E(\pi_{acc})$ = −0.03 [−0.08] eV}. Based on the interaction diagram it is concluded that the main shift for π_c in going from **9** to **1** has to be attributed to an inductive shift.

Although a (small) interaction between the olefinic bond and the groups at the termini has now been demonstrated, this is not yet the case for interaction between the anilino moiety and the dicyanoethylene acceptor. In order to probe this direct interaction the following steps (not shown in the figure) were performed. All NBO's were allowed to interact with the exception of all NBO's forming the Lp–π_{ar} system. Values found: π_c = −9.42; π_{acc} = −10.42 eV. Comparison of these values with those of step 6 leads to the conclusion that the direct TBI effect of the anilino moiety on the energy of the acceptor is only 0.02 eV. The effect of the acceptor on the energy levels of the anilino π system are evaluated by allowing all NBO's to interact with the exception of the π_{acc} PCMO. This results in the following energy levels: π_c = −9.44, π_{ar}–Lp = −8.15, π_{ar} = −9.27, Lp–π_{ar} = −10.78 eV. Comparison with the values for step 6 shows that the TBI influence of the acceptor on the energy levels of the anilino π system does not exceed 0.01 eV. The direct interaction between the π systems of the donor and that of the acceptor thus is in the order of 0.01 eV.

Effects of the geometry around N in 1 on TBI. A similar interaction diagram was obtained for **1** optimized in C_s symmetry (Supplementary Data, Fig. 4S) as for **1** in C_1 symmetry. The C_s geometry largely corresponds to the geometry found for **1** in the crystal (see above). Due to the optimal alignment of the Lp with respect to the phenyl π system, the Lp–π interaction in **1** (C_s) is enlarged compared to **1** (C_1), giving a splitting between the π_{ar}–Lp and Lp–π_{ar} levels of 4.17 eV (C_s) instead of 3.38 eV in **1** (C_1) in step 2. As a result of the lower lying Lp–π_{ar} level TBI with π_c is reduced moderately compared to **1** {step 3 to 4 [5 to 6]: ΔE(Lp–π_{ar}) = −0.06 [−0.07] eV for **1** (C_s) *versus* −0.07 [−0.09] eV for **1**}, while the TBI between π_c and π_{acc} is concomitantly increased {step 3 to 4 [5 to 6]: $\Delta E(\pi_{acc})$ = −0.05 [−0.10] eV for **1** (C_s) *versus* −0.03 [−0.08] eV for **1**}. Thus the NBO analyses indicate that TBI between phenyl N and π_c in the lowest energy C_1 conformer and in the closely related C_s symmetric conformer of **1** are very small and almost identical.

A different picture arises for C_s symmetric **1** in which the phenyl group is rotated by 90° (Supplementary Data, Fig. 5S). In this conformation, **1** ⊥ (C_s), †† the phenyl π system is oriented orthogonal to the nitrogen lone pair so that Lp–π_{ar} interaction is absent (step 2). As a result, upon interaction with all σ NBO's the energies of the Lp PCMO (−8.71 eV) and the π_c PCMO (−8.74 eV) are nearly identical (step 3), bringing about a considerable TB splitting in going to step 4 {$\Delta[E(\text{Lp}) - E(\pi_c)]$ = 0.45 eV}. Upon admixture of all antibonding and Rydberg orbitals the TB splitting between Lp and π_c in going from 5 to 6 is reduced {$\Delta[E(\text{Lp}) - E(\pi_c)]$ = 0.30 eV}, while the interaction with π_{acc} is slightly increased {step 3 to 4 [5 to 6]: $\Delta E(\pi_{acc})$ = −0.06 eV [−0.10 eV]}.

A similar test for the occurrence of direct TBI between the anilino donor and the dicyanoethylene acceptor as for **1** was performed. Omission of the Lp–π_{ar} NBO's gives the following energies: π_c = −9.36; π_{acc} = −10.39. Omission of the π_{acc} NBO's gives: π_c/Lp = −9.25; π_{ar} = −9.14; Lp/π_c = −9.81. Comparison of these values with those of step 6 shows that, even though the TBI between the Lp and π_c is very large in **1** ⊥ (C_s), the direct interaction between the Lp and the acceptor does not exceed 0.01 eV.

From the interaction schemes of **1**, **1** (C_s) and **1** ⊥ (C_s) it can be concluded that rotation of the phenyl group has a pronounced effect on the TBI between π_c and the anilino π system. When going from **1** ⊥ (C_s) to **1** the Lp–π_{ar} PCMO is less stabilized (step 2), while the interaction with the σ NBO's is increased (step 3). In effect, upon further rotation, the energy level of the Lp–π_{ar} PCMO will approach and eventually cross that of the π_c PCMO. The increased interaction with the σ skeleton and the improved energy matching with the π_c PCMO will increase TBI between the Lp and π_c. Due to the minor effect on the energy of the π_c level, TBI between π_c and π_{acc} is hardly affected by rotation around the N–phenyl bond. It can therefore be concluded that, according to our calculations, this low energy barrier process {E[**1** ⊥ (C_s)] − E(**1**) = 0.9 kcal mol^{-1}}, should be able to temporarily increase the ground state electronic interaction between the anilino moiety and the double bond substantially.

It has been found[13] that an axial orientation of the phenyl group in **3** significantly increases the intensity of the CT absorption. Since this should originate from a better ground state donor–acceptor coupling, it is of interest to investigate the ground state TBI of **1** with an axial phenyl group. At the RHF/6-31G level of theory, however, all attempts to find a minimum for the axial conformer failed. Only when imposing a C_s symmetry constraint, could a transition state (see the Experimental section) be found for the axial conformer, which is only 3.0 kcal mol^{-1} higher in energy than the fully optimized geometry. ‡‡[28] As can be seen in going from step 3 to 4 and from 5 to 6 in the interaction scheme of **1** ax (C_s) (Supplementary Data, Fig. 6S) the ground state TBI between π_c and both the Lp–π_{ar} level and the π_{ar}–Lp level is increased compared to **1** (C_1) and **1** (C_s). While the absolute numbers remain low {step 3 to 4 [5 to 6]: $\Delta E(\pi_{ar}\text{–Lp})$ = 0.04 eV [0.05 eV] and ΔE(Lp–π_{ar}) = −0.07 eV [−0.13 eV]}, the increase relative to **1** (C_1) is significant.

†† RHF/6-31G calculations revealed this to be a minimum (see Experimental section).

‡‡ At the B3LYP/6-31G level of theory the axial conformer of **4** could be optimized.[28] It was found to be only 0.79 kcal mol^{-1} higher in energy than the equatorial conformer.

The results presented here indicate that rotational states of the phenyl group, which modulate the energy of the π_{ar}–Lp and the Lp–π_{ar} levels, may be very important for the ground state TBI between donor and acceptor in molecules such as **1** and **3**. Processes which depend strongly on such TBI, such as CT absorption and charge recombination of the excited CT state, may thus be strongly affected by rotation of the phenyl group.

NBO analysis of 2. The NBO interaction diagram of **2** (fully optimized geometry; C_1 symmetry) is given in the Supplementary Data (Fig. 7S). Steps 1 to 3 are similar to those in **1** (C_1) (Fig. 8) albeit that π_c is absent. Step 4 reveals that TBI is virtually absent in this compound despite the good match of the Lp–π_{ar} and π_{acc} energies. The presence of the π bond thus is essential to mediate TBI between the anilino donor and the dicyanoethylene acceptor. Rotation around the C–N bond placing the π system orthogonal to the lone pair on nitrogen does not change this picture (Supplementary Data, Fig. 8S).

Structural consequences of TBI in 1 and 2

There is a discussion in literature as to whether TBI can cause appreciable bond lengthening of C–C bonds.[29] It has been claimed[13] that the length of a C–C bond participating in TBI between a donor and an acceptor can be increased by 0.02 Å due to TBI. In **1** such a bond would be the C(10)–C(11) bond.[9a,10] While in **1** a TBI between the olefinic bond and the dicyanoethylene acceptor is present as concluded from the NBO analyses (see above) and as is also evident from the presence of an intramolecular CT absorption in **11** and a related compound,[4a,30] in **6** any TBI between the olefinic bond and the carbonyl group is expected to be very small.[10] As concluded from the NBO analyses TBI between the dicyanoethylene acceptor and the *N*,*N*-dialkylanilino chromophore **2** is negligibly small. Moreover, a CT absorption is not observed in **2**.[5] For **1**, **2** and **6** the C(10)–C(11) bond lengths amount to 1.5523(15), 1.540(2) and 1.519(4)–1.529(4) Å, respectively. For the parent compound of **1** and **6**, *viz.* 1,1′-bi(cyclohexylidene) (**9**) the corresponding (mean) bond length is 1.530(2) Å.[31] The longest bond is the one in **1**, which seems to be consistent with the occurrence of TBI in this compound. It is however not clear whether TBI is responsible for the full 0.01–0.02 Å difference, since such a small TBI is not expected to give this difference. Moreover, more factors may contribute to the observed bond lengthening.

Another geometrical consequence of TBI between an electron donor and the dicyanoethylene acceptor would be the pyramidalization of the C(12) atom.[13] This would occur in such a way that the acceptor would point in an axial direction with a positive angle Θ (defined in Fig. 2). In the absence of TBI the acceptor would point in an equatorial direction (negative Θ). Values of Θ were found to vary between +8 (largest TBI) and −5° (no TBI). For **1** and **2** these values are +1 and −4°. This would indicate a small TBI in **1** between the olefinic bond and the acceptor and no TBI in **2**, which is in agreement with predictions.

Conclusions

In the crystal structures of **1** and **2** intermolecular electron-donor–acceptor complexes are formed. As a result, a clear intermolecular CT absorption is observed in the solid state which is either very weak and of an intramolecular nature (**1**) or not present at all (**2**) in the solution spectra. It is therefore concluded that in the crystal intermolecular TS orbital interaction dominates over TB orbital interaction. Complex formation finds expression in a twist of the phenyl group in **1** and **2** in order to optimize contact between the π systems of the anilino moiety and the dicyanoethylene acceptor.

PES results correlate well with RHF/6-31G calculations and indicate that the energy levels of **1** and **2** are hardly affected by TBI. NBO analyses support this conclusion. Furthermore, the NBO analyses indicate that there is a small but distinct TBI between the olefinic bond and the dicyanoethylene acceptor on one hand (order of 0.2 eV) and between the olefinic bond and the anilino donor on the other (order of 0.1 eV). The latter is significantly affected by rotation of the phenyl group around the C–N bond. An axial orientation of the *N*,*N*-dialkylanilino donor may also increase TBI with the π_e orbital as compared to the equatorial conformer. The effect is, however, much smaller than that of rotation. Direct ground state TBI between the anilino donor and the acceptor in **1** is hardly detectable (order of 0.01 eV). The same holds for **2**.

Furthermore, TB effects obtained by only allowing bonding NBO's to interact do not account for all TBI. Thus, in the RHF/6-31G NBO description of TBI the σ* and/or Rydberg NBO's are also of importance.

Structural consequences of TBI between the olefinic π bond and the anilino donor or the dicyanoethylene acceptor as bond lengthening and pyramidalization in the acceptor may be present in **1**.

Experimental

The syntheses of compounds **1**,[4a] **2**,[4a] **4**,[4a] **5**[32] and **8**[4a] are described elsewhere.

X-Ray crystal structure determination of 1 and 2§§

Crystals of **1** and **2** suitable for X-ray analysis were obtained by slow evaporation of a solution (1.0 mg mL^{-1}) in CH_2Cl_2–ethyl acetate (1 : 1 v/v) at 20 °C. Crystals were glued to a Lindemann-glass capillary and transferred into the cold nitrogen stream on a Nonius KappaCCD diffractometer. Data sets were measured using graphite monochromated Mo-Kα radiation ($\lambda = 0.71073$ Å) from a rotating anode source. Pertinent data for the structure determinations are collected in Table 1. Both structures were solved by direct methods, using SHELXS86[33] for compound **1** and SHELXS97[34] for compound **2**, and refined on F^2, using full-matrix least-squares techniques (SHELXL-97-2[35]). Hydrogen atoms were located on a difference Fourier map and their co-ordinates were refined. The non-hydrogen atoms were refined with anisotropic thermal parameters, hydrogen atoms were refined with a fixed isotropic displacement parameter related to the value of the equivalent isotropic displacement parameter of their carrier atoms by a factor of 1.2. Neutral atom scattering factors and anomalous dispersion corrections were taken from the International Tables for Crystallography.[36]

Solid state UV–Vis absorption spectroscopy

Solid state UV–Vis diffuse reflectance spectra were recorded on a Varian Cary5 UV–Vis-NIR spectrophotometer equipped with a Harrick Praying Mantis diffuse reflectance accessory. Reflectance ordinates R were transformed into Kubelka Munk units $F(R)$ by $F(R) - (1 - R)^2/2R$.

He (I) photoelectron spectroscopy

He (I) PE spectra were recorded on a Perkin Elmer PS 18 spectrometer at the following temperatures T/°C: **1**: 200; **4**: 100; **5**: 60 and **8**: 90. Calibration was performed with Ar (15.76 and 15.94 eV) and Xe (12.13 and 13.44 eV). Resolution was 20 meV on the $^2P_{\frac{3}{2}}$ Ar line.

Ab initio calculations

All quantum mechanical calculations were run on a Silicon

§§ CCDC reference numbers 160667 and 160668. See http://www.rsc.org/suppdata/p2/b1/b102410h/ for crystallographic data files in .cif or other electronic format.

Graphics Power Challenge and Origin 2000 computer using GAMESS-UK.[37] Geometries were optimized at the RHF/6-31G level of theory [cartesian coordinates files are available upon request (L. W. J.)]. The total RHF/6-31G energies (in hartree) obtained were: **1**: −932.514877; **1** (C_s): −932.511006; **1** ⊥ (C_s): −932.513730; **1** ax (C_s): −932.510103; **2**: −933.697564; **2** (C_s): −933.693658; **2** ⊥ (C_s): −933.696255; **2** ax (C_s): −933.693090; **4**: −711.306125; **5**: −595.411714; **5** (C_s): −595.408199; **7**: −479.541747; **8**: −712.488276; **10**: −349.978403; **11** (C_s): −687.084442; NBO analyses were done using the NBO 3.0 program[38] as implemented in GAMESS-UK. Second derivatives for **1** and **2** were numerically calculated at the RHF/6-31G level of theory. The geometries of **1** (C_s) (−67.4 cm^{-1}), **1** ax (C_s) (−48.0 cm^{-1}), **2** (C_s) (−78.7 cm^{-1}) and **2** ⊥ (C_s) (−19.2 cm^{-1}) were characterized as transition states for rotation around the phenyl C–N bond. The geometry of **2** ax (C_s) was found to be a transition state both for rotation around the phenyl C–N bond (−56.9 cm^{-1}) and for the axial–equatorial motion of the phenyl group (−26.7 cm^{-1}) and **1** ⊥ (C_s) was found to be a minimum.

Acknowledgements

A. Flatow (University of Heidelberg) is gratefully acknowledged for recording the PE spectra. This research (W. D. O. and, in part, A. L. S.) has been financially supported by the Council for Chemical Sciences of the Netherlands Organization for Scientific Research (CW-NWO). The work in Heidelberg was supported by the Deutsche Forschungsgemeinschaft, the Fonds der Chemischen Industrie and the BASF Aktiengesellschaft in Ludwigshafen.

References

1 *Introduction to Molecular Electronics*, eds. M. C. Petty, M. R. Bryce and D. Bloor, Edward Arnold, London, 1995.
2 M. R. Wasielewski, *Chem. Rev.*, 1992, **92**, 435; R. A. Marcus and N. Sutin, *Biochim. Biophys. Acta*, 1985, **811**, 265.
3 N. Koga, K. Sameshima and K. Morokuma, *J. Phys. Chem.*, 1993, **97**, 13117; L. A. Curtiss, C. A. Naleway and J. R. Miller, *J. Phys. Chem.*, 1995, **99**, 1182; K. D. Jordan and M. N. Paddon-Row, *Chem. Rev.*, 1992, **92**, 395; M. J. Shephard, M. N. Paddon-Row and K. D. Jordan, *J. Am. Chem. Soc.*, 1994, **116**, 5328; M. N. Paddon-Row, *Acc. Chem. Res.*, 1994, **27**, 18; M. N. Paddon-Row and M. J. Shephard, *J. Am. Chem. Soc.*, 1997, **119**, 5355.
4 (*a*) F. J. Hoogesteger, C. A. Walree, L. W. Jenneskens, M. R. Roest, J. W. Verhoeven, W. Schuddeboom, J. J. Piet and J. M. Warman, *Chem. Eur. J.*, 2000, **6**, 2948; (*b*) R. J. Willemse, PhD Thesis, University of Amsterdam, Amsterdam, The Netherlands, 1997.
5 F. J. Hoogesteger, R. W. A. Havenith, J. W. Zwikker, L. W. Jenneskens, H. Kooijman, N. Veldman and A. L. Spek, *J. Org. Chem.*, 1995, **60**, 4375.
6 F. J. Hoogesteger, J. M. Kroon, L. W. Jenneskens, E. J. R. Sudhölter, T. J. M. de Bruin, J. W. Zwikker, E. ten Grotenhuis, C. H. M. Marée, N. Veldman and A. L. Spek, *Langmuir*, 1996, **12**, 4760.
7 F. J. Hoogesteger, L. W. Jenneskens, H. Kooijman, N. Veldman and A. L. Spek, *Tetrahedron*, 1996, **52**, 1773; A. W. Marsman, E. D. Leussink, J. W. Zwikker, L. W. Jenneskens, W. J. J. Smeets, N. Veldman and A. L. Spek, *Chem. Mater.*, 1999, **11**, 1484.
8 E. P. A. M. Bakkers, A. L. Roest, A. W. Marsman, L. W. Jenneskens, L. I. de Jong-van Steensel, J. J. Kelly and D. Vanmaekelbergh, *J. Phys. Chem. B*, 2000, **104**, 7266; E. P. A. M. Bakkers, A. W. Marsman, L. W. Jenneskens and D. Vanmaekelbergh, *Angew. Chem.*, 2000, **112**, 2385; E. P. A. M. Bakkers, A. W. Marsman, L. W. Jenneskens and D. Vanmaekelbergh, *Angew. Chem., Int. Ed.*, 2000, **39**, 2297.
9 (*a*) A. W. Marsman, R. W. A. Havenith, S. Bethke, L. W. Jenneskens, R. Gleiter, J. H. van Lenthe, M. Lutz and A. L. Spek, *J. Org. Chem.*, 2000, **65**, 4584; (*b*) R. W. A. Havenith, PhD Thesis, Utrecht University, Utrecht, The Netherlands, 2000.
10 A. W. Marsman, R. W. A. Havenith, S. Bethke, L. W. Jenneskens, R. Gleiter and J. H. van Lenthe, *Eur. J. Org. Chem.*, 2000, 2629.
11 D. Cremer and J. A. Pople, *J. Am. Chem. Soc.*, 1975, **97**, 1354.
12 H. Kooijman, A. L. Spek, F. J. Hoogesteger and L. W. Jenneskens, *Acta Crystallogr., Sect. C: Cryst. Struct. Commun.*, 1997, **53**, 1156.
13 B. Krijnen, H. B. Beverloo, J. W. Verhoeven, C. A. Reiss, K. Goubitz and D. Heijdenrijk, *J. Am. Chem. Soc.*, 1989, **111**, 4433.
14 K. Ogawa, J. Harada, M. Endo and Y. Takeuchi, *Tetrahedron Lett.*, 1997, **38**, 5663.
15 M. D. Rozeboom, K. N. Houk, S. Searles and S. E. Seyedrezai, *J. Am. Chem. Soc.*, 1982, **104**, 3448.
16 T. Dahl, *Acta Chem. Scand.*, 1994, **48**, 95; K. Müller-Dethlefs and P. Hobza, *Chem. Rev.*, 2000, **100**, 143.
17 A. I. Kitaigorodskii, *Organic Chemical Crystallography*, Consultants Bureau, New York, 1961, p. 106.
18 A. L. Spek, PLATON, A Multipurpose Crystallographic Tool (http://www.cryst.chem.uu.nl/platon/), Utrecht University, Utrecht, The Netherlands, 2001.
19 W. D. Oosterbaan, C. Koper, T. W. Braam, C. A. van Walree and L. W. Jenneskens, unpublished work.
20 T. Koopmans, *Physica*, 1934, **1**, 104.
21 (*a*) G. Häfelinger, C. U. Regelmann, T. M. Krygowski and K. Wozniak, *J. Comput. Chem.*, 1989, **10**, 329; (*b*) F. J. Hoogesteger, J. H. van Lenthe and L. W. Jenneskens, *Chem. Phys. Lett.*, 1996, **259**, 178; (*c*) R. W. A. Havenith, L. W. Jenneskens and J. H. van Lenthe, *Chem. Phys. Lett.*, 1998, **282**, 39.
22 J. P. Maier and D. W. Turner, *J. Chem. Soc., Faraday Trans. 2*, 1973, **69**, 521; S. A. Cowling and R. A. W. Johnstone, *J. Electron Spectrosc. Relat. Phenom.*, 1973, **2**, 161.
23 (*a*) R. Hoffmann, P. D. Mollère and E. Heilbronner, *J. Am. Chem. Soc.*, 1973, **95**, 4860; (*b*) E. Heilbronner, E. Honegger, W. Zambach, P. Schmitt and H. Günther, *Helv. Chim. Acta*, 1984, **67**, 1681.
24 P. Pasman, J. W. Verhoeven and T. J. de Boer, *Tetrahedron*, 1976, **32**, 2827.
25 R. Hoffmann, *Acc. Chem. Res.*, 1971, **4**, 1.
26 E. Heilbronner and A. Schmelzer, *Helv. Chim. Acta*, 1975, **58**, 936; A. E. Reed and F. Weinhold, *J. Chem. Phys.*, 1983, **78**, 4066; A. E. Reed, R. B. Weinstock and F. Weinhold, *J. Chem. Phys.*, 1985, **83**, 735; A. Imamura and M. Ohsaku, *Tetrahedron*, 1981, **37**, 2191.
27 M. N. Paddon-Row, S. S. Wong and K. D. Jordan, *J. Chem. Soc., Perkin Trans. 2*, 1990, 425.
28 W. D. Oosterbaan, M. Koeberg, J. Piris, C. A. van Walree, B. R. Wegewijs, L. W. Jenneskens and J. W. Verhoeven, *J. Phys. Chem. A*, 2001, in the press.
29 K. K. Baldridge, T. R. Battersby, R. VernonClark and J. S. Siegel, *J. Am. Chem. Soc.*, 1997, **119**, 7048.
30 P. Pasman, F. Rob and J. W. Verhoeven, *J. Am. Chem. Soc.*, 1982, **104**, 5127.
31 N. Veldman, A. L. Spek, F. J. Hoogesteger, J. W. Zwikker and L. W. Jenneskens, *Acta Crystallogr., Sect. C: Cryst. Struct. Commun.*, 1994, **50**, 742.
32 F. J. Hoogesteger, PhD Thesis, Utrecht University, Utrecht, The Netherlands, 1996.
33 G. M. Sheldrick, SHELXS86, Program for Crystal Structure Determination, University of Göttingen, 1986.
34 G. M. Sheldrick, SHELXS97, Program for Crystal Structure Determination, University of Göttingen, 1997.
35 G. M. Sheldrick, SHELXL-97-2, Program for Crystal Structure Refinement, University of Göttingen, 1997.
36 A. J. C. Wilson, *International Tables for Crystallography, Volume C*, Kluwer Academic Publishers, Dordrecht, The Netherlands, 1992.
37 GAMESS-UK is a package of *ab initio* programs written by M. F. Guest, J. H. van Lenthe, J. Kendrick, K. Schoffel, P. Sherwood and R. J. Harrison, 2000, with contributions from R. D. Amos, R. J. Buenker, M. Dupuis, N. C. Handy, I. H. Hillier, P. J. Knowles, V. Bonacic-Koutecky, W. von Niessen, V. R. Saunders and A. J. Stone. The package is derived from original GAMESS code by M. Depuis, D. Spangler and J. Wendolowski, NRCC Software Catalog, Vol. 1, Program No. QG01 (GAMESS), 1980.
38 E. D. Glendening, A. E. Reed, J. E. Carpenter and F. Weinhold, NBO 3.0 Program: Natural Bond Orbital/Natural Population Analysis/Natural Localized Molecular Orbitals Program, as implemented in GAMESS-UK[37] (see also ref. 26).